

Investigating Peptide-Coenzyme A Conjugates as Chemical Probes for Proteomic Profiling of N-Terminal and Lysine Acetyltransferases

Julia Sindlinger,^[a] Stefan Schön,^[a] Jürgen Eirich,^[b] Sören Kirchgäßner,^[a] Iris Finkemeier,^{*,[b]} and Dirk Schwarzer^{*,[a]}

Acetyl groups are transferred from acetyl-coenzyme A (Ac-CoA) to protein N-termini and lysine side chains by N-terminal acetyltransferases (NATs) and lysine acetyltransferases (KATs), respectively. Building on lysine-CoA conjugates as KAT probes, we have synthesized peptide probes with CoA conjugated to N-terminal alanine (α -Ala-CoA), proline (α -Pro-CoA) or tri-glutamic acid (α -3Glu-CoA) units for interactome profiling of NAT complexes. The α -Ala-CoA probe enriched the majority of NAT catalytic and auxiliary subunits, while a lysine CoA-conjugate

bound only a subset of endogenous KATs. Interactome profiling with the α -Pro-CoA probe showed reduced NAT recruitment in favor of metabolic CoA binding proteins and α -3Glu-CoA steered the interactome towards NAA80 and NatB. These findings agreed with the inherent substrate specificities of the target proteins and showed that N-terminal CoA-conjugated peptides are versatile probes for NAT complex profiling in lysates of physiological and pathological backgrounds.

Introduction

The majority of eukaryotic proteins are subjected to N-terminal acetylation.^[1] This modification is installed post- or co-translationally, either at the initial methionine (iMet) residue or the residue following iMet after its removal by methionine aminopeptidases (Figure 1a).^[2] The latter occurs most frequently at N-terminally released serine and alanine residues, but is not restricted to these sites. Recent studies uncovered that N-terminal acetylation is a means of proteome stabilization by masking of N-terminal degron sequences.^[3] This modification is installed by N-terminal acetyltransferases (NATs) that exist in the seven major protein complexes NatA to NatF and NatH in mammalian cells.^[1,4] NatA is responsible for N-terminal acetylation after iMet removal and contains NAA10 as catalytic subunit as well as NAA15, NAA50, and HYPK.^[5] The remaining NATs acetylate N-terminal iMet depending on the downstream residues (NatB, NatC, NatE, and NatF) or are specific for individual proteins such as histones or actin (NatD and NatH).^[5,6]

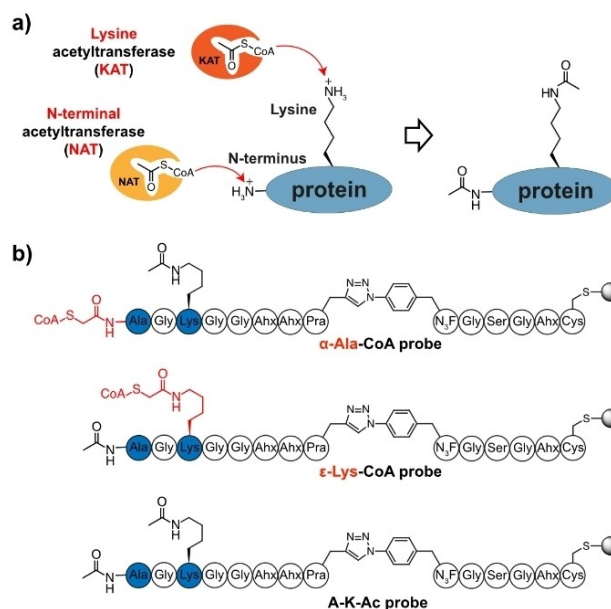


Figure 1. a) Cellular proteins are subjected to acetylation at their N-termini and lysine side chains. The corresponding reactions are catalyzed by N-terminal acetyltransferases (NATs) and lysine acetyltransferases (KATs). b) Design of chemical proteomic probes for NATs and KATs. The amino acid composition of all three probes is identical consisting of an N-terminal fraction including reciprocally CoA-conjugated and acetylated amino group at the N-terminus and the lysine side chain (α -Ala-CoA and ϵ -Lys-CoA). The A-K-Ac control probe is acetylated at both amino groups. The probes contain a C-terminal fragment installed after CoA conjugation by 'click chemistry' adding a thiol moiety for covalent immobilization on solid support. Abbreviations: 6-Amino-hexanoic acid (Ahx), Propargylglycine (Pra), 4-Azidophenylalanine (N₃F).

[a] Dr. J. Sindlinger, S. Schön, Dr. S. Kirchgäßner, Prof. Dr. D. Schwarzer
Interfaculty Institute of Biochemistry (IFIB)
University of Tübingen
Auf der Morgenstelle 34, 72076 Tübingen (Germany)
E-mail: dirk.schwarzer@uni-tuebingen.de

[b] Dr. J. Eirich, Prof. Dr. I. Finkemeier
Institute of Plant Biology and Biotechnology
University of Münster
Schlossplatz 7, 48149 Münster (Germany)
E-mail: finkemeier@uni-muenster.de

Supporting information for this article is available on the WWW under <https://doi.org/10.1002/cbic.202200255>

© 2022 The Authors. ChemBioChem published by Wiley-VCH GmbH. This is an open access article under the terms of the Creative Commons Attribution Non-Commercial NoDerivs License, which permits use and distribution in any medium, provided the original work is properly cited, the use is non-commercial and no modifications or adaptations are made.

In addition to N-terminal acetylation, proteins are subjected to posttranslational lysine acetylation, catalyzed by lysine acetyltransferases (KATs).^[7] KATs have been initially discovered

as histone acetyltransferases,^[8] but lysine acetylation profiling analyses revealed that they possess a broad set of histone and non-histone substrates in the nucleus and other cellular compartments (Figure 1a).^[9] KATs are grouped into the major families: p300/CBP, GCN5, MYST, and NCOA and are also commonly imbedded as catalytic subunits into multi-protein complexes.^[7,10] KATs have been recognized as drug targets^[11] and the first reported KAT inhibitor – Lys-CoA – was established as chemical probe for dissecting the catalytic properties of KAT p300/CBP.^[12] This inhibitor is a conjugate of Coenzyme A (CoA) and the N ϵ -amide of N-acetyl-lysine bridged by an acetyl spacer, thereby serving as bisubstrate-KAT-inhibitor. Imbedding the CoA-conjugated lysine residue into peptide sequences derived from KAT substrate sites allowed altering the specificity of this type of probe towards individual KATs.^[12] NATs utilize the same co-substrate – Ac-CoA – as KATs and share the superfamily of GCN5-related N-acetyltransferases with KAT family members (Figure 1a). Consequently, N-terminal CoA conjugated peptides including the acetyl-spacer have been established as bisubstrate-inhibitors of recombinant and immunoprecipitated endogenous NATs.^[13] The N-terminal residue was shown to modulate the efficiency of the tested inhibitors in agreement with the NAT substrate specificity. Furthermore, bisubstrate-analogs were used as tools for structural elucidations of NAT complexes.^[14]

Both, NATs and KATs and their respective protein complexes are highly relevant in physiological processes and diseases. Consequently, tools for monitoring changes in NAT and KAT abundance, activity and complex composition are in high demand. Activity-based protein profiling (ABPP) is an attractive strategy for this purpose.^[15] A typical ABPP probe consists of a reactive chemical moiety, referred to as warhead, that binds to the active site of the target enzyme, a linker group which can be used for tuning the specificity of the probe and a reporter tag. The reporter tag is frequently used for enriching the target enzymes from cellular lysates, enabling subsequent analysis and quantification by mass spectrometry (MS). In general, ABPP is used in cellular lysates and targets endogenous proteins in native modification states and in contact with interaction partners. This type of chemoproteomics approach has already been used for investigating KATs by adopting the concept of CoA bisubstrate inhibitors for ABPP.^[16] The corresponding Lys-CoA probes were equipped with a photo-crosslinking group and a 'clickable' handle for subsequent attachment of fluorophores and biotin tags and allowed KAT profiling in cancer cell lysates. In addition, immobilized Lys-CoA was used for chemical proteomics profiling of KAT complexes by high-resolution mass spectrometry.^[17] KATs have further been shown to bind CoA-derived probes enabling proteome-wide KAT substrate profiling.^[18] However, immobilized Lys-CoA probes did not enrich all of mammalian KATs from cellular lysates. Furthermore, the probe also bound NATs and metabolic enzymes possessing acetyl-CoA binding sites.^[17a] In general, pull-downs from cellular lysates will not enrich proteins on the bases of probe-affinity alone, but the abundance of the protein plays an important role as well. As a result, interaction profiles can change with proteome adjustments to environmental changes, which pro-

vides valuable information about redundancies of related proteins. On the other hand, this complicates determining the specificity of the probes towards endogenous enzymes. With recombinant proteins, Lys-CoA derivatives serve as potent KAT inhibitors with reported IC₅₀s in the high nanomolar range.^[12] A major hurdle for addressing the question of peptide-CoA conjugate specificity in cellular lysates is the lack of interactome data obtained with probes designed to target the competing NAT enzymes in direct comparison to data obtained with KAT-targeting probes.

In this investigation we wanted to establish immobilized peptide-CoA conjugates for targeting endogenous NATs in native cellular lysates by chemoproteomics profiling. At the same time, we wanted to explore the ability of these probes to discriminate between KATs and NATs and how probe design impacts targeting of individual NAT complexes. The obtained data should further enable ABPP of NAT and KAT complexes in health and disease models.

Results and Discussion

The central determinant distinguishing NAT from KAT activity is the substrate amino group in a peptide probe. Here we investigated if installing the CoA-conjugate at the N α or the N ϵ amine is sufficient for discriminating between NATs and KATs by interactome profiling. Proteins with N-terminal Ala residues are most commonly acetylated by NATs. Consequently, the first NAT probe contained an N-terminal Ala residue for installing the CoA-conjugate. The probe design further contained a Lys residue for alternative N ϵ installation of the CoA-conjugate in probes targeting KATs. In order to explore if the site of CoA-conjugation is sufficient for discriminating between NATs and KATs, the probe design featured only Gly residues and amino-hexanoic acid (Ahx) spacers, which should not enforce the probe-protein interactions to a large extent. The synthesis strategy prohibits the installation of Cys residues, commonly used for peptide immobilization, because the thiol would compete with CoA in the conjugation reaction. We installed a C-terminal propargylglycine (Pra) instead of Cys in order to introduce an anchoring thiol by azide-alkyne cycloaddition after the CoA conjugation reaction. Three probes were synthesized based on this design (Figure 1b): The α -Ala-CoA probe contained CoA installed at the N-terminus and acetylated Lys (CoA-Ala-Gly-Lys(Ac)-Gly-Gly-Ahx-Ahx-Pra). The KAT-targeting ϵ -Lys-CoA probe was acetylated at the N-terminus, while the lysine side chain was conjugated to CoA (Ac-Ala-Gly-Lys(CoA)-Gly-Gly-Ahx-Ahx-Pra). A control probe (A-K-Ac) with acetylated N-terminus and Lys side chain Ac-Ala-Gly-Lys(Ac)-Gly-Gly-Ahx-Ahx-Pra) completed the set (Figure 1b). Probe peptides were synthesized and conjugated to CoA based on reported procedures.^[12,13,16,19] Briefly, after solid-phase synthesis of probe peptides and deprotection of the N α – or N ϵ - amines, bromoacetic acid was installed at the respective sites. The peptides were cleaved off the solid support and CoA was conjugated to the electrophilic bromoacetyl group in solution (Supporting Figure S1). A thiol handle for immobilization was installed by

Table 1. Enrichment of main NAT and KAT catalytic subunits in N-CoA vs. N-K-Ac, K-CoA vs. N-K-Ac, and N-CoA vs. K-CoA experiments. * $p < 0.05$; ** $p < 0.01$; *** $p < 0.005$ ($n = 3$, LIMMA test statistics).

Enzyme type	Enzyme name	\log_2 -fold change N-CoA/N-K-Ac	\log_2 -fold change K-CoA/N-K-Ac	\log_2 -fold change N-CoA/K-CoA
Catalytic subunit of NATs	NAA10	4.85***	1.96***	2.89***
	NAA20	4.17***	0.03	4.15***
	NAA30	3.07***	2.30***	0.77**
	NAA40	2.24***	1.71***	0.53
	NAA50	5.18***	4.45***	0.73**
	NAA80	1.42***	2.13***	-0.71**
Catalytic subunit of KATs	KAT7 (HBO1)	0.56*	2.45***	-1.89***
	KAT8 (MOF1)	0.04	3.72***	-3.68***
	ATAT1	0.66*	4.71***	-3.71***
	ESCO2	1.98***	3.35***	-0.91
	KAT2A (hGCN5)	-0.06	0.87***	-0.91***
	CBP (CREBBP)	0.59*	0.79*	-0.20

Further enriched proteins bind nucleotides like ATP, AMP, or NAD^+ , indicating that the specificity of the probes for acetyltransferases is not absolute. These include strongly enriched 5-formyltetrahydrofolate cyclo-ligase (MTHFS), which could be recruited to α -Ala-CoA by direct interactions with the nucleotide fraction of the probe. Alternatively, these proteins could represent so far unknown NAT binding partners (Figure 2a). Proteins significantly enriched on ϵ -Lys-CoA versus A-K-Ac are illustrated in the volcano plot of Figure 2b, showing proteins significantly enriched on ϵ -Lys-CoA in the upper right section. These proteins include lysine acetyltransferases ESCO2, ATAT1, KAT7, KAT8, and KAT2 A (Figure 2b). Enrichment of these KATs from HeLa lysates is in agreement with previous reports using Sepharose-bound Lys-CoA and lysine-CoA conjugates derived from histones H3 and H4.^[17a] We further identified paralog KATs p300/CBP (KAT3a/KAT3b) which were weakly enriched on ϵ -Lys-CoA (CBP was found significantly enriched on ϵ -Lys-CoA, but not p300). The \log_2 -fold enrichments of KATs were stronger for the ϵ -Lys-CoA probe when compared to the experiment with the α -Ala-CoA bait. This pattern was preserved with KAT binding proteins like JADE4 and ING4, which are part of the KAT7/HBO1 complex. We further identified proteins containing acetyl-lysine-binding bromodomains like BRD4, but these proteins showed no consistent enrichment pattern supporting the notion that binding modules of acetylated lysine residues are not enriched on this probe (Table S1). Some of the catalytic and auxiliary subunits of NAT complexes were enriched on ϵ -Lys-CoA. These include NAA10, NAA30, NAA40, NAA50, and NAA80. Enrichment ratios of catalytic NAT subunits were lower on ϵ -Lys-CoA when compared with α -Ala-CoA, indicating preferred interaction with the α -Ala-CoA probe (Table 1).

Plotting the interactome of α -Ala-CoA against the interactome of ϵ -Lys-CoA illustrated the preferences of both probes towards their target proteins (Figure 2c). Proteins significantly enriched on α -Ala-CoA over ϵ -Lys-CoA localize to the upper-right section of the plot with positive \log_2 -fold changes. Proteins enriched more strongly on ϵ -Lys-CoA than on α -Ala-CoA appear in the upper left section with negative \log_2 -fold

changes. Binders of CoA-conjugates with no preference to the site of CoA attachment are located in the center of the plot (Figure 2c). The strongest enriched proteins of α -Ala-CoA were components of the NatA/E and NatB complexes (NAA10, NAA15, NAA16, NAA20, and NAA25). The plot further showed strong α -Ala-CoA-enrichment of NatA component HypK, which serves as regulator of NatA and NatE activity.^[5b,14a] The NatC components, NAA30 and NAA35, are also located in the upper right section of the volcano plot (Figure 2c). The only NAT component located in the left section of preferred ϵ -Lys-CoA binders was NAA80. This catalytic subunit acetylates poly-acidic N-termini of processed actin and might be less compatible with an N-terminal alanine residue as CoA attachment site.^[4] KATs and KAT-binding proteins appear in the upper left section of the plot and are indicating stronger interactions with ϵ -Lys-CoA than α -Ala-CoA. The strongest enriched proteins of ϵ -Lys-CoA were the catalytic KATs KAT8, ATAT1, and KAT7 indicating a strong impact of the CoA attachment site on KAT recognition. We further observed that several non-protein acetyltransferases and CoA binding proteins, like glucosamine 6-phosphate N-acetyltransferase (GNPNAT1), acyl coenzyme A thioester hydrolase (ACOT7), and ATP-citrate synthase (ACLY) are found on the left-hand side of the plot indicating preferred binding of the lysine CoA conjugate. Assuming that these proteins bind via the nucleotide fraction of the probe, this finding could be explained by the lower steric hindrance of CoA attached to the lysine side chain amine when compared to the $\text{N}\alpha$ amine linkage of the N-terminal attachment site. This interpretation could imply that chemical proteomics with this particular set of NAT probes might be less susceptible to off-target protein binding than KAT probes, but variations in cellular abundances and activity of individual KATs and NATs will most likely impact the probe interactomes as well. N-terminal acetylation occurs largely co-translationally by ribosome associated NAT complexes in the cytoplasm.^[1] However, posttranslational N-terminal acetylation is also subject of current investigations, when N-termini are cleaved such as after organellar import.^[23] Lysine acetylation is installed in the nucleus and the cytoplasm by KATs located in the respective compartments or KATs shuttling between

cytoplasm and nucleus. In order to investigate the impact of NAT and KAT localization and the resulting changes in protein abundances on α -Ala-CoA and ϵ -Lys-CoA binding we determined their interactomes in the nuclear (NE) and cytoplasmic (CE) fractions of HeLa lysates (Supporting Figure S2). Volcano plots of α -Ala-CoA versus ϵ -Lys-CoA interactomes in nuclear and cytoplasmic extract showed similar patterns as observed in whole cell lysates (Supporting Figure S3). Components of the NatA and NatB complexes were the strongest enriched proteins of the α -Ala-CoA probe when compared to ϵ -Lys-CoA and A-K-Ac in experiments with NE and CE (Supporting Tables S2 and S3). Catalytic NAA10 is a very low abundant protein in NE and its strong enrichment from nuclear extracts indicates a high degree of specificity to the α -Ala-CoA probe (Supporting Figure S2). KATs were enriched on ϵ -Lys-CoA from NE and CE (Supporting Figure S3). KAT8 belongs to the nuclear KATs and was consequently only detected and quantified in experiments with NE.^[24] In contrast, KAT7 was found enriched on ϵ -Lys-CoA in experiments with CE which is in agreement with its localization in both compartments (Supporting Figure S4).^[25] KAT7 was also the only KAT ranking among the strongest ϵ -Lys-CoA enriched proteins in any of these experiments, corroborating the notion that the α -Ala-CoA probe possess a higher degree of specificity for their target proteins than the ϵ -Lys-CoA probe.

We validated the interactions of selected endogenous NATs and KATs with α -Ala-CoA, ϵ -Lys-CoA, and the A-K-Ac control by Western Blot analysis. In agreement with the above-detected specificity, KAT7 showed binding of ϵ -Lys-CoA and only weak interactions with α -Ala-CoA and A-K-Ac (Figure 3a and Supporting Figure S2b). NAA10 and NAA25 showed exclusive recruitment to α -Ala-CoA from CE. NAA50 was recruited to α -Ala-CoA and with apparent weaker affinity to ϵ -Lys-CoA as well (Fig-

ure 3a and Supporting Figure S2b). These findings are in agreement with the chemical proteomics experiments of α -Ala-CoA and ϵ -Lys-CoA.

Encouraged by these findings, we continued exploring the specificity of $N\alpha$ -conjugated peptide probes for targeting individual NAT complexes. The NatA complex is mainly responsible for N-terminal acetylation after iMet removal, which is reflected in the strongest fold-change enrichments of catalytic subunits NAA10 and NAA50 on α -Ala-CoA. However, NatA is not reported to acetylate all protein N-termini after iMet removal and prominent examples are proteins with N-terminal Pro residue, which are not subjected to N-terminal acetylation.^[26] A surprising finding of the chemoproteomics profiling was NAA80, which enriched only poorly on α -Ala-CoA and even preferentially interacted with the ϵ -Lys-CoA probe (Figure 2c). NAA80 is a specialized N-terminal acetyltransferase and acetylates the N-termini of β - and γ -actin, reflected in the in vitro preference for substrates with N-terminal Asp and Glu residues.^[27] Hence, we synthesized two further N-CoA peptide conjugates with either Pro (α -Pro-CoA) or a tri-Glu (α -3Glu-CoA) sequence at the N-terminus (Figure 4a). The probes were synthesized and immobilized as before, followed by LC-MS/MS analyses of pull-down experiments from native HeLa cell lysates in comparison with pull-downs with α -Ala-CoA and A-K-Ac probes (Supporting Table S4).

The volcano plot of the proteins enriched on α -Pro-CoA versus the A-K-Ac control showed enrichment of the main catalytic NATs and a few KATs on α -Pro-CoA (Figure 4b). However, the fold-change in enrichment of these proteins was significantly lower when compared to the α -Ala-CoA probe. This effect is also evident when plotting the enrichments on α -Pro-CoA against α -Ala-CoA, showing depletion of all NATs and KATs from α -Pro-CoA, which is in line with the notion that none of these proteins serve as N-Pro acetyltransferases (Figure 4c). In contrast to acetyltransferases, we observed enrichment of enzymes involved in CoA metabolism on α -Pro-CoA. In particular pantothenate kinase like protein PANK4 stood out as the most strongly enriched protein (Figure 4c). The biochemistry of PANK4 is not fully understood, but unlike other pantothenate kinases this protein possesses 4'-phosphopantetheine phosphatase activity.^[28] Acetyltransferase activity has not been reported for pantothenate kinase, but they can bind to acetyl-CoA as part of a feedback inhibition mechanism that modulates cellular CoA levels.^[29] It appears plausible that PANK4 can bind to α -Pro-CoA as a result of reduced competition from NATs via its acetyl-CoA binding site.

The interactome of the α -3Glu-CoA probe showed strong enrichment of catalytic NATs NAA20 and NAA80 (Figure 4d). Plotting the enrichments on α -3Glu-CoA against α -Ala-CoA showed that both of these NATs and the auxiliary NAA25 interacted preferentially with α -3Glu-CoA in contrast to other NATs (Figure 4e). The interaction profile of NAA80 mirrors its enzymatic specificity as acetyltransferase of β/γ -actin possessing Asp/Glu rich N-termini. NAA20 and NAA25 form the NatB complex that commonly acetylates proteins with N-terminal iMet residue. However, in contrast to the NatC, NatE, and NatF complexes, which also modify iMet, NatB prefers an Asx/Glx

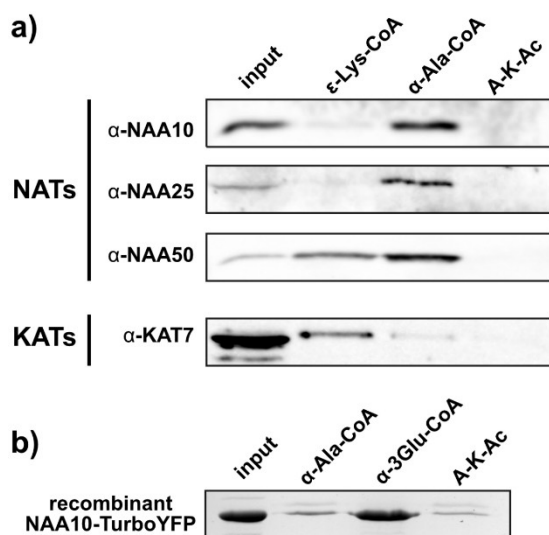


Figure 3. a) Western Blot validation of selected NAT and KAT proteins. KAT7 and NAA10 were analyzed in whole cell extract (WCE) and NAA25 and NAA50 in cytosolic extract (CE). The input signal corresponds to 16 μ g or 32 μ g of the respective HeLa extracts. b) SDS-PAGE analysis of pull-down experiments with recombinant NAA10-TurboYFP (5 μ M).

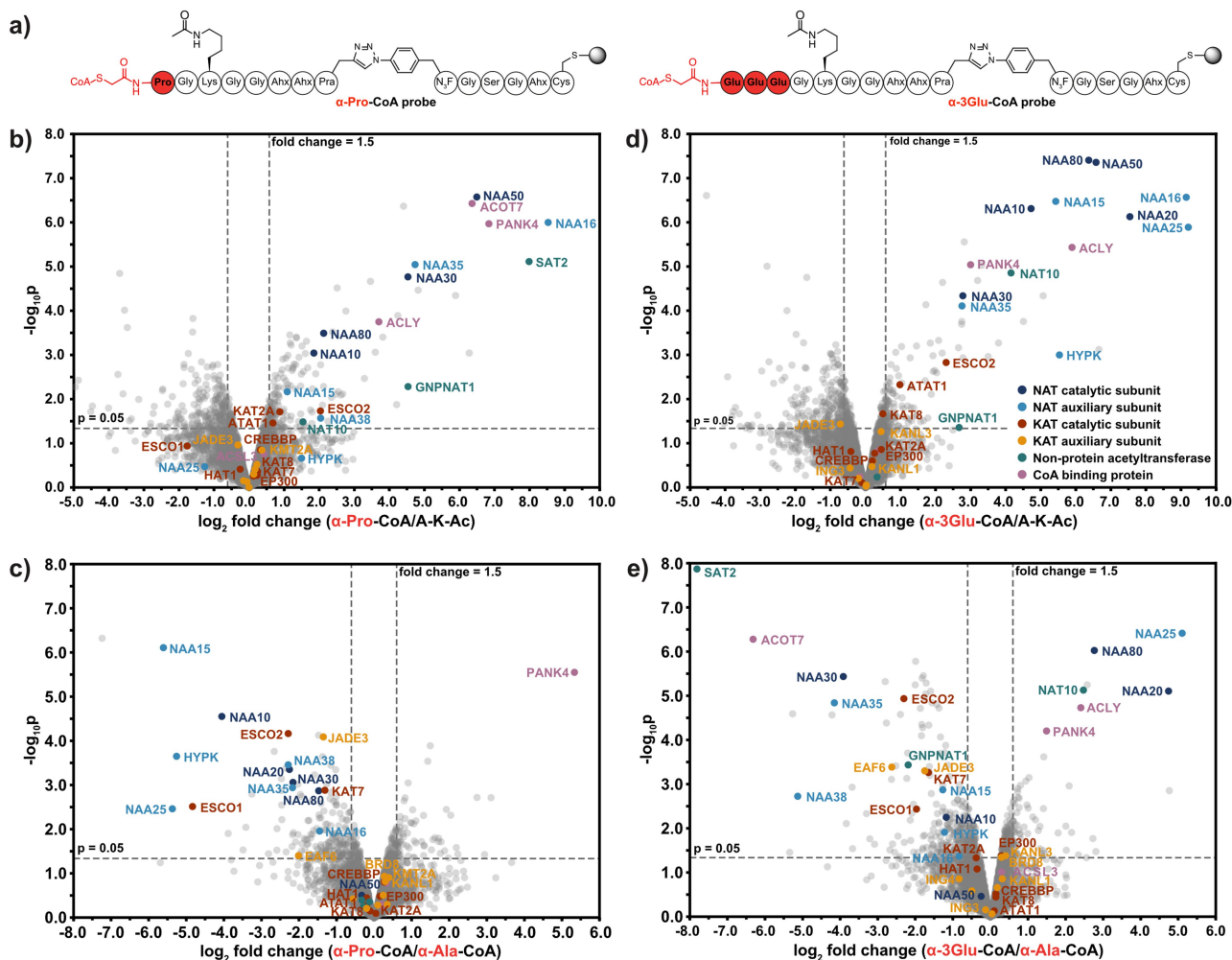


Figure 4. Probe structures and volcano plots of experiments with α -Pro-CoA and α -3Glu-CoA a) Design of α -Pro-CoA and α -3Glu-CoA probes. Volcano plots of: b) α -Pro-CoA versus A-K-Ac, c) α -Pro-CoA versus α -Ala-CoA, d) α -3Glu-CoA versus A-K-Ac, and e) α -3Glu-CoA versus α -Ala-CoA enriched proteins from HeLa whole cell extract (WCE). \log_2 -fold changes of proteins enriched on probes over controls are plotted against $-\log p$ from experiments in triplicate ($n = 3$). Dotted lines indicate cut-offs of $p < 0.05$ and enrichment > 1.5 -fold.

residue downstream of iMet, which is provided by the α -3Glu-CoA probe.^[1] The volcano plot in Figure 4 further shows catalytic NAA10 enriched on α -Ala-CoA over α -3Glu-CoA, which is consistent with the reported substrate specificity for N-terminal Ala and Ser residues.^[1,30] However, this specificity only applies for NAA10 imbedded into the NatA complex, whereas free NAA10 was shown to acetylate acidic N-termini.^[30] In order to investigate if the peptide-CoA conjugates can also readout this shift in NAA10's substrate selectivity we performed pull-down experiments with NAA10 recombinantly expressed in *E. coli* as TurboYFP fusion. The experiment showed indeed poor interaction with α -Ala-CoA and the N-K-Ac control, while NAA10-TurboYFP was efficiently retained on the α -3Glu-CoA probe (Figure 3b). These findings indicate that the major fraction of NAA10 in the HeLa cell lysate is imbedded in the NatA complex.

Collectively, the observations support the notion that the substrate specificity of NATs translates into the peptide-CoA interactomes in chemoproteomics profiling experiments.

Conclusion

In summary, we have investigated the specificity of CoA-peptide conjugates for profiling of NATs and KATs. The α -Ala-CoA probe enriched the majority of catalytic and a broad set of auxiliary NAT domains from HeLa lysate. Importantly, catalytic and auxiliary subunits of NATs were among the strongest enriched proteins when compared to the A-K-Ac control probe. These findings were made with whole cell lysates, cytosolic fractions and even nuclear extracts where NAT abundance is commonly low. In contrast, the ϵ -Lys-CoA probe recruited only a subset of known KATs from HeLa lysates and a broader set of binding proteins. Western blot analysis confirmed these findings for selected NATs and KATs, supporting the notion that N-terminal CoA conjugates are more efficient probes for targeting NATs when compared to Lys-CoA probes for interactome profiling of KATs. We further refined the N-terminal CoA conjugates with the aim to target individual NATs more precisely. NAA80 is a specialized NAT with the acidic N-termini

of β/γ -actin as exclusive substrates and was only poorly enriched on α -Ala-CoA. The α -3Glu-CoA probe recruited NAA80 efficiently, reflecting its inherent substrate specificity. Proteins of the NatB complex also favored α -3Glu-CoA over α -Ala-CoA in agreement with their specificity for acidic residues downstream of iMet. NATs acetylating N-Pro residues have not been discovered yet, which is reflected in the diminished NAT recruitment to the α -Pro-CoA probe. However, reduced NAT recruitment is accompanied by enhanced recruitment of CoA-binding proteins, in particular PANK4, indicating that probe design can be adapted to targeting CoA-binding proteins. The strong enrichment of PANK4 on α -Pro-CoA is still surprising and might point to other yet undiscovered functions of this protein. In general, peptide probes with N-terminal CoA conjugates appear as powerful tools for profiling of NAT complexes in different tissues or during diseases, and even provide the ability of finetuning the specificity for individual NAT complexes. These probes could now be used for chemoproteomics profiling of changes in NAT complex abundance and composition upon biological perturbation like disease onset and progression or NAT inhibitor treatment.

Experimental Section

Materials: Standard amino acid derivatives for solid-phase peptide synthesis and 2-(1*H*-benzotriazol-1-yl)-1,1,3,3-tetramethyluronium hexafluorophosphate (HBTU) were purchased from GL Biochem (Shanghai, China). Fmoc-6-Ahx-OH and Fmoc-Pra-OH were bought from IRIS Biotech (Marktredwitz, Germany), Boc-p-azido-Phe-OH and Fmoc Lys(Ac) OH from Bachem (Bubendorf, Switzerland), *N*-succinimidyl bromoacetate from TCI Chemicals (Eschborn, Germany) and Coenzyme A (CoA) trilithium salt from Sigma-Aldrich (Steinheim, Germany). Other chemicals were obtained from Sigma-Aldrich, Merck (Darmstadt, Germany), Carl Roth (Karlsruhe, Germany), TCI Chemicals, Bachem or Carbolution (St. Ingbert, Germany). Organic solvents were purchased from J. T. Baker (Deventer, Netherlands), VWR (Leuven, Belgium), Fisher Scientific (Loughborough, UK), Biosolve (Valkenswaard, Netherlands) and Th. Geyer (Renningen, Germany).

General methods: Preparative peptide purifications were performed on a Varian ProStar 210 HPLC device endowed with a Reprosil C18 column (250×20 mm, 5 μ m, 100 Å, Dr. Maisch, Ammerbuch, Germany) with solvents HPLC-A (0.1% trifluoroacetic acid (TFA) in water) and HPLC B (80% ACN, 0.1% TFA in water). The applied gradient was 5 to 95% HPLC-B in 40 min with a flow rate of 13 mL/min. The gradient was monitored by absorption at 218 nm. Fractions were collected manually, afterwards analyzed by LC-MS, and lyophilized.

Liquid chromatography-mass spectrometry (LC-MS) was performed on a LC-MS 2020 system from Shimadzu (Kyoto, Japan) equipped with a Kinetex C18 column (100×2.1 mm, 2.6 μ m, 100 Å, Phenomenex, Aschaffenburg, Germany). Samples were prepared with solvent LCMS-A (0.1% formic acid (FA) in water) and LCMS-B (80% ACN, 0.1% FA in water). The flow rate was 0.2 mL/min with a gradient from 5 to 95% LCMS-B within 12.75 min. Absorption was detected at 218 nm and the ESI-MS was operated in positive mode.

Solid-phase peptide synthesis (SPPS): Peptides were synthesized based on solid-phase peptide synthesis (SPPS) by the Fmoc/tBu strategy on TentaGel R RAM or HL RAM resins (Rapp Polymere, Tübingen, Germany), with loading capacity of 0.38 mmol/g as solid

support. Syntheses were performed on 25 μ mol scale and the automated peptide synthesis was carried out on a Syro I synthesizer from MultiSynTech GmbH (Witten, Germany). Standard amino acid building blocks were protected at the side chains as follows: Cys(Trt), Lys(Boc), Ser(tBu). Coupling reactions of amino acid building blocks (3 eq with respect to the resin) were performed twice. The first coupling reactions were performed with *N,N'*-diisopropylcarbodiimid (DIC) (3 eq) and ethyl cyanohydroxyiminoacetate (Oxyma Pure) (3 eq) in DMF for 40 min, followed by coupling with HBTU (3 eq) with 300 mM *N*-methylmorpholine (NMM) in DMF for 30 min. The Fmoc group was deprotected with 40% piperidine in DMF two times for 3 min.

N-terminal acetylation of the peptides was accomplished by incubating the resin with a solution of 0.6 mL acetic anhydride, 0.6 mL *N,N*-diisopropylethylamine and 2.8 mL DMF for 20 min while shaking. This step was repeated once, afterwards the resin was washed with DMF (3×1 min).

Coupling of the *N*-succinimidyl bromoacetate was performed on resin, followed by washing with 400 mM NMM in DMF. 4 eq *N*-succinimidyl bromoacetate in anhydrous DCM were incubated with the resin for 1 h under argon and gentle agitation. This step was repeated once. The bromoacetylation reactions for probe peptides α -Pro-CoA and α -3Glu-CoA were performed by incubating the resin with 5 eq 2-bromoacetic anhydride in anhydrous DMF for 30 minutes under argon while shaking. The reaction was repeated once.

Cleavage of crude peptides was carried out with 10 mL of cleavage solution containing TFA, phenol, triisopropylsilane (TIPS) and water (85:5:5:5) under shaking for 3 h. The supernatant was concentrated under reduced pressure and crude peptides were precipitated in cold diethyl ether (40 mL), centrifuged (4000×g, 10 min, -4°C), dissolved in water, and lyophilized. Peptides were purified by preparative HPLC and analyzed by LC-MS (Supporting Figure S5).

CoA conjugation: Conjugation with CoA was performed by incubating bromoacetylated peptides dissolved in 0.5 mL of 1 M triethylammonium bicarbonate buffer (Sigma-Aldrich) at pH 8.5 and 5 eq CoA trilithium salt.^[12] The reaction mixture was stirred under argon at room temperature for 24 h. The mixture was acidified with TFA to pH 3–4 before HPLC purification (Supporting Figure S6).

Copper catalyzed alkyne azide cycloaddition: The azido-phenyl-alanine peptide (4 μ mol), alkyne peptides (3 μ mol), CuSO₄·5 H₂O (12 μ mol) and ascorbic acid (2.2 mmol) were mixed in water and dimethyl sulfoxide (DMSO) (7:3 v/v). Tris((1-benzyl-4-triazolyl)methyl)amine (TBTA) (12 μ mol) dissolved in DMSO was added and the reaction was incubated over night at room temperature. Afterwards the mixture was purified by preparative HPLC. In order to prevent undesired disulfide formation 0.5 mmol tris(2-carboxyethyl)phosphine (TCEP) was added to the purified peptide prior to lyophilization (Supporting Figure S7).

Peptide immobilization: SulfoLink Coupling Resin suspension (300 μ L for each peptide) (Thermo Fisher Scientific, Rockford, USA) was drained and washed with coupling buffer (50 mM Tris·HCl, 5 mM EDTA-Na, pH 8.5) (5×800 μ L).^[31] 300 μ L of the peptide solution (1 mM in coupling buffer) were added and the resin was incubated at room temperature for 1 h. After washing with coupling buffer (3×500 μ L), 500 μ L of blocking buffer (50 mM β mercaptoethanol in coupling buffer) were added to each resin and incubated for 1 h. Afterwards, the resin was washed with 1 M NaCl solution (6×1 mL), water (2×1 mL) and 50% ACN in water (4×1 mL). The dry resin was mixed with 450 μ L of 50% ACN in water, aliquots of 40 μ L were prepared and stored at -20°C.

Further experimental procedures are provided in the Supporting Information.

Acknowledgements

We are grateful for financial support by the Deutsche Forschungsgemeinschaft (DFG) with grants SCHW 1163/9-1, INST 211/744-1 FUGG and FI 1655/4-1. Open Access funding enabled and organized by Projekt DEAL.

Conflict of Interest

The authors declare no conflict of interest.

Data Availability Statement

Raw data of LC-MS/MS analysis is deposited on the jPOST server and available for download under the identifiers JPST001556 (<https://repository.jpostdb.org/entry/JPST001556.3>) for Pro and Glu probes and JPST000827 (<https://repository.jpostdb.org/entry/JPST000827.0>) for samples related to Ala and Lys related probes.

Keywords: acetylation · chemoproteomics · coenzyme A · lysine acetyltransferase · N-terminal acetyltransferase

- [1] H. Aksnes, A. Drazic, M. Marie, T. Arnesen, *Trends Biochem. Sci.* **2016**, *41*, 746–760.
- [2] a) A. Breiman, S. Fieulaine, T. Meinnel, C. Giglione, *Biochim. Biophys. Acta* **2016**, *1864*, 531–550; b) C. Giglione, S. Fieulaine, T. Meinnel, *Biochimie* **2015**, *114*, 134–146.
- [3] a) E. Linster, F. L. Forero Ruiz, P. Miklankova, T. Ruppert, J. Mueller, L. Armbruster, X. Gong, G. Serino, M. Mann, R. Hell, M. Wirtz, *Nat. Commun.* **2022**, *13*, 810; b) F. Mueller, A. Friese, C. Pathe, R. C. da Silva, K. B. Rodriguez, A. Musacchio, T. Bange, *Sci. Adv.* **2021**, *7*, eabc8590.
- [4] M. Goris, R. S. Magin, H. Foyn, L. M. Myklebust, S. Varland, R. Ree, A. Drazic, P. Bhambra, S. I. Stove, M. Baumann, B. E. Haug, R. Marmorstein, T. Arnesen, *Proc. Natl. Acad. Sci. USA* **2018**, *115*, 4405–4410.
- [5] a) T. Arnesen, K. K. Starheim, P. Van Damme, R. Evjenth, H. Dinh, M. J. Betts, A. Rynningen, J. Vandekerckhove, K. Gevaert, D. Anderson, *Mol. Cell. Biol.* **2010**, *30*, 1898–1909; b) S. Deng, N. McTiernan, X. Wei, T. Arnesen, R. Marmorstein, *Nat. Commun.* **2020**, *11*, 818.
- [6] H. Aksnes, R. Ree, T. Arnesen, *Mol. Cell* **2019**, *73*, 1097–1114.
- [7] B. N. Sheikh, A. Akhtar, *Nat. Rev. Genet.* **2019**, *20*, 7–23.
- [8] J. E. Brownell, C. D. Allis, *Proc. Natl. Acad. Sci. USA* **1995**, *92*, 6364–6368.
- [9] T. Narita, B. T. Weinert, C. Choudhary, *Nat. Rev. Mol. Cell Biol.* **2019**, *20*, 156–174.
- [10] K. K. Lee, J. L. Workman, *Nat. Rev. Mol. Cell Biol.* **2007**, *8*, 284–295.
- [11] a) D. R. Friedmann, R. Marmorstein, *FEBS J.* **2013**, *280*, 5570–5581; b) R. Marmorstein, *J. Mol. Biol.* **2001**, *311*, 433–444.
- [12] O. D. Lau, T. K. Kundu, R. E. Soccio, S. Ait-Si-Ali, E. M. Khalil, A. Vassilev, A. P. Wolffe, Y. Nakatani, R. G. Roeder, P. A. Cole, *Mol. Cell* **2000**, *5*, 589–595.
- [13] H. Foyn, J. E. Jones, D. Lewallen, R. Narawane, J. E. Varhaug, P. R. Thompson, T. Arnesen, *ACS Chem. Biol.* **2013**, *8*, 1121–1127.
- [14] a) F. A. Weyer, A. Gumiero, K. Lapouge, G. Bange, J. Kopp, I. Sinning, *Nat. Commun.* **2017**, *8*, 15726; b) G. Liszczak, J. M. Goldberg, H. Foyn, E. J. Petersson, T. Arnesen, R. Marmorstein, *Nat. Struct. Mol. Biol.* **2013**, *20*, 1098–1105.
- [15] a) A. B. Berger, P. M. Vitorino, M. Bogoy, *Am. J. Pharmacogenomics* **2004**, *4*, 371–381; b) K. T. Barglow, B. F. Cravatt, *Nat. Methods* **2007**, *4*, 822–827; c) B. F. Cravatt, A. T. Wright, J. W. Kozarich, *Annu. Rev. Biochem.* **2008**, *77*, 383–414; d) J. Krysiak, R. Breinbauer, *Top. Curr. Chem.* **2012**, *324*, 43–84.
- [16] D. C. Montgomery, A. W. Sorum, J. L. Meier, *J. Am. Chem. Soc.* **2014**, *136*, 8669–8676.
- [17] a) D. C. Montgomery, J. M. Garlick, R. A. Kulkarni, S. Kennedy, A. Allali-Hassani, Y. M. Kuo, A. J. Andrews, H. Wu, M. Vedadi, J. L. Meier, *J. Am. Chem. Soc.* **2016**, *138*, 6388–6391; b) D. C. Montgomery, A. W. Sorum, L. Guasch, M. C. Nicklaus, J. L. Meier, *Chem. Biol.* **2015**, *22*, 1030–1039.
- [18] a) Y. Hwang, P. R. Thompson, L. Wang, L. Jiang, N. L. Kelleher, P. A. Cole, *Angew. Chem. Int. Ed.* **2007**, *46*, 7621–7624; *Angew. Chem.* **2007**, *119*, 7765–7768; b) M. He, Z. Han, L. Liu, Y. G. Zheng, *Angew. Chem. Int. Ed.* **2018**, *57*, 1162–1184; *Angew. Chem.* **2018**, *130*, 1176–1199.
- [19] L. Schmohl, D. Schwarzer, *J. Pept. Sci.* **2014**, *20*, 145–151.
- [20] J. Cox, M. Mann, *Nat. Biotechnol.* **2008**, *26*, 1367–1372.
- [21] J. Cox, M. Y. Hein, C. A. Luber, I. Paron, N. Nagaraj, M. Mann, *Mol. Cell. Proteomics* **2014**, *13*, 2513–2526.
- [22] a) J. S. Akella, D. Wloga, J. Kim, N. G. Starostina, S. Lyons-Abbott, N. S. Morrisette, S. T. Dougan, E. T. Kipreos, J. Gaertig, *Nature* **2010**, *467*, 218–222; b) T. Nishiyama, R. Ladurner, J. Schmitz, E. Kreidl, A. Schleiffer, V. Bhaskara, M. Bando, K. Shirahige, A. A. Hyman, K. Mechtler, J. M. Peters, *Cell* **2010**, *143*, 737–749.
- [23] T. V. Dinh, W. V. Bienvenut, E. Linster, A. Feldman-Salit, V. A. Jung, T. Meinnel, R. Hell, C. Giglione, M. Wirtz, *Proteomics* **2015**, *15*, 2426–2435.
- [24] K. C. Neal, A. Pannuti, E. R. Smith, J. C. Lucchesi, *Biochim. Biophys. Acta* **2000**, *1490*, 170–174.
- [25] C. Zou, Y. Chen, R. M. Smith, C. Snavely, J. Li, T. A. Coon, B. B. Chen, Y. Zhao, R. K. Mallampalli, *J. Biol. Chem.* **2013**, *288*, 6306–6316.
- [26] R. Ree, S. Varland, T. Arnesen, *Exp. Mol. Med.* **2018**, *50*, 1–13.
- [27] a) A. Drazic, H. Aksnes, M. Marie, M. Boczkowska, S. Varland, E. Timmerman, H. Foyn, N. Glomnes, G. Rebowski, F. Impens, K. Gevaert, R. Dominguez, T. Arnesen, *Proc. Natl. Acad. Sci. USA* **2018**, *115*, 4399–4404; b) E. Wiame, G. Tahay, D. Tyteca, D. Vertommen, V. Stroobant, G. T. Bommer, E. Van Schaftingen, *FEBS J.* **2018**, *285*, 3299–3316.
- [28] L. Huang, A. Khusnutdinova, B. Nocek, G. Brown, X. Xu, H. Cui, P. Petit, R. Flick, R. Zallot, K. Balmant, M. J. Ziemak, J. Shanklin, V. de Crecy-Lagard, O. Fiehn, J. F. Gregory, 3rd, A. Joachimiak, A. Savchenko, A. F. Yakunin, A. D. Hanson, *Nat. Chem. Biol.* **2016**, *12*, 621–627.
- [29] B. S. Hong, G. Senisterra, W. M. Rabeh, M. Vedadi, R. Leonardi, Y. M. Zhang, C. O. Rock, S. Jackowski, H. W. Park, *J. Biol. Chem.* **2007**, *282*, 27984–27993.
- [30] P. Van Damme, R. Evjenth, H. Foyn, K. Demeyer, P. J. De Bock, J. R. Lillehaug, J. Vandekerckhove, T. Arnesen, K. Gevaert, *Mol. Cell. Proteomics* **2011**, *10*, M110004580.
- [31] J. Seidel, T. Meisinger, J. Sindlinger, P. Pieloch, I. Finkemeier, D. Schwarzer, *ChemBioChem* **2019**, *20*, 3001–3005.

Manuscript received: May 2, 2022

Revised manuscript received: July 1, 2022

Accepted manuscript online: July 1, 2022

Version of record online: July 25, 2022